Lee and Lee *Micro and Nano Syst Lett* (2019) 7:9
https://doi.org/10.1186/s40486-019-0088-3

Micro and Nano Systems Letters

LETTER Open Access

Beyond mass measurement for single microparticles via bimodal operation of microchannel resonators

Bong Jae Lee and Jungchul Lee*

Abstract

This paper reports bimodal operation of microchannel resonators towards measurements of properties associated with energy dissipation resulting from travelling particles along with their buoyant masses. Two independent actuation methods are applied for simultaneous operation of the first and second flexural bending modes of cantilever-type microchannel resonators. The first mode is operated in closed loop feedback and the second mode is operated in open loop. During a single microparticle transit inside a microchannel resonator, resonance frequency of the first mode is measured via a heterodyne frequency down-mixer and amplitude and phase of the second mode are measured via a lock-in technique. While a 5-μm diameter single polystyrene particle is dynamically trapped by alternating pneumatic pressure gradient, frequency shift of the first mode and amplitude change and phase shift of the second mode are measured, analyzed, and then statistically compared. Bimodal operation of microchannel resonators demonstrated herein can be applicable to arbitrary modes and will be useful to provide information associated with energy dissipation in addition to buoyant mass for particles of interest.

Keywords: Bimodal operation, Dynamic trapping, Energy dissipation, Microchannel resonators

Background

Suspended microchannel resonators (SMRs) [1] are novel microfluidic microelectromechanical systems (MEMS) devices that are basically mechanical resonators with an integrated microfluidic channel. High quality factor resulting from vacuum packaging facilitates single particle and cell measurements with high resolution by monitoring the resonance frequency shift precisely. Since cantilever-type (clamped-free) SMRs operated at their fundamental resonance frequencies exhibit the position-dependent measurement error near the free end, the second flexural mode has been exploited to measure buoyant masses of particles at antinodes [2]. This is because the channel width typically wider than the traveling particle imposes the transversal position uncertainty for antinode positions but the longitudinal position uncertainty for the tip position. Since SMRs are narrow and long in general, the longitudinal position uncertainty predominantly affects the frequency noise. Recently, a similar concept was further extended to extract buoyant masses and positions of travelling objects by employing phase-locked loop operation of multiple vibration modes simultaneously [3]. Although such a demonstration is promising to identify and track a specific one out of multiple particles co-travelling within a suspended region of the resonator, amplitude change and phase shift of a specific vibration mode closely related with energy dissipation were not measured or recorded.

Dynamic (or AC) mode atomic force microscopy (AFM) [4], a forefather technique of SMRs, relies on an oscillating cantilever. Via dynamic mode AFM, useful information such as amplitude change or phase shift in addition to the surface topography could be obtained. Two representative dynamic AFM modes are amplitude modulation AFM (AM-AFM) [4] in air or liquid environments and frequency modulation AFM (FM-AFM) [5] in vacuum.

*Correspondence: jungchullee@kaist.ac.kr
Department of Mechanical Engineering, Korea Advanced Institute of Science and Technology, 291 Daehak-ro, Yuseong-gu, Daejeon 34141, Republic of Korea

Considering the simple feedback operation, AM-AFM, also known as tapping mode AFM, is more frequently used. AM-AFM has initially used the fundamental resonance frequency [4, 6] and explored higher modes later on since higher modes can offer better phase contrast than the first mode [7]. For simultaneous dynamic mode topography and phase contrast mapping of one or more higher modes, the fundamental mode AM-AFM is performed along with additional excitations of constant amplitude and frequency near specific higher modes [8]. In general, such a technique is called multifrequency imaging [9–11]. When the total number of modes associated is two, it becomes dual frequency or bimodal AFM [12–16]. If the bimodal operation providing information associated with energy dissipation, stiffness, and elastic modulus besides topography is applied to SMRs, information other than buoyant mass of particles may be investigated. This promising idea, however, has not been demonstrated yet.

Experimental details

Mode characteristics

When a particle suspended in a buffer travels through the cantilever (clamped-free) type microchannel resonator, frequency responses depend on the characteristic mode shape as shown in Fig. 1. The schematic in Fig. 1a shows a microchannel resonator with its cover removed for clarification. Mode shapes and associated mass responsivities for the first and second modes are displayed in Fig. 1b and expected time-dependent variation of the first and second mode resonance frequencies are shown in Fig. 1c while the particle travels through the integrated channel. When the suspended particle enters and leaves the suspended region of the microchannel resonator, monotonic and non-monotonic mass responsivities of the first and second modes result in one and three characteristic peaks, respectively. From the Euler–Bernoulli beam equation, mode shapes are given by

$$u_n\left(\frac{x}{l}\right) = \frac{A_n}{2}\left[\left(\cosh\left(\frac{\lambda_n x}{l}\right) - \cos\left(\frac{\lambda_n x}{l}\right)\right) - \left(\frac{\cosh\lambda_n + \cos\lambda_n}{\sinh\lambda_n + \sin\lambda_n}\right) \times \left(\sinh\left(\frac{\lambda_n x}{l}\right) - \sin\left(\frac{\lambda_n x}{l}\right)\right)\right] \quad (1)$$

In this paper, bimodal operation of suspended microchannel resonators are explored with two independent actuations for the first time. The first flexural mode driven by integrated electrostatic actuation is operated in closed loop feedback and the second flexural mode driven by off-chip piezo actuator is operated in open loop. The closed loop operation keeps track of the resonance frequency and makes a microchannel resonator run at its resonance frequency all the time and the open loop operation measures amplitude change and phase shift by using AC drive with constant frequency and amplitude. This bimodal operation is applied to a 5-μm diameter single polystyrene particle travelling back and forth by alternating pneumatic pressure.

where x is the position from the clamped edge, l is the suspended length of the cantilever, A_n is the oscillation amplitude at the free end, and λ_n is the eigenvalue for the nth eigenmodes. With $A_n = 1$ (normalized mode shape), relative resonance frequency shift of the cantilever with an added mass of Δm is formulated by applying (1) to the Rayleigh–Ritz theorem as follows

$$\left(\frac{\Delta f}{f}\right)_n = -1 + \left[1 + u_n\left(\frac{x}{l}\right)^2 \cdot \frac{\Delta m}{m_{eff}}\right]^{-1/2} \quad (2)$$

where f is the resonance frequency and m_{eff} is the effective mass.

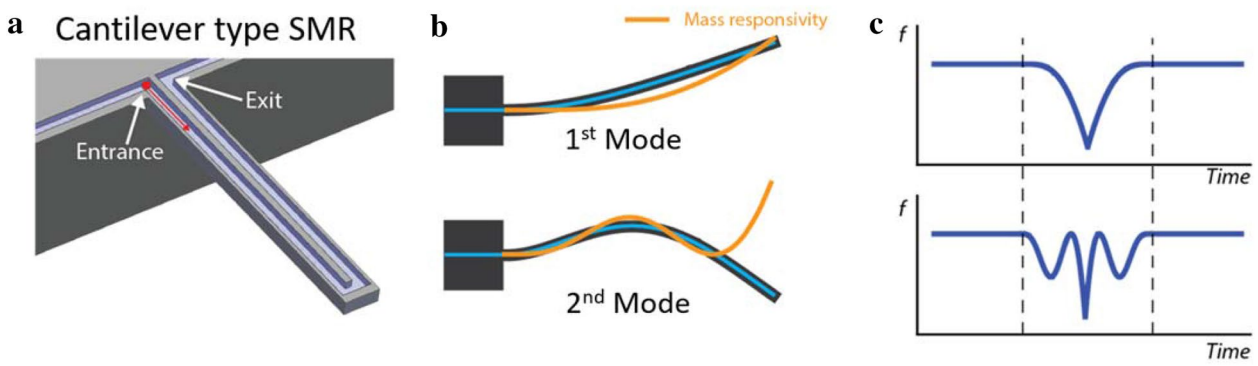

Fig. 1 Mode characteristics and frequency responses of cantilever (clamped-free) type suspended microchannel resonators (SMRs) with a traveling particle. **a** Schematic of a cantilever-type SMR with its top cover removed. **b** Mode shape and associated mass responsivity of the resonance frequency of the first and second flexural bending modes. **c** Variation of the first and second mode resonance frequencies while a particle travels through the integrated channel

Open and closed loop operation

In general, resonators can be operated in open or closed loop. For open loop operation, a resonator is excited at a fixed frequency and magnitude near its resonance frequency (see Fig. 2a, right). When the resonance frequency is shifted due to any reason (e.g. position change of a particle), amplitude change and phase shift are induced simultaneously (see Fig. 2a, left). Such induced responses can be simply measured by using a lock-in amplifier. For closed loop operation, a resonator is always running at its resonance frequency by feeding measured amplitude response back to actuation (see Fig. 2b, right). When the resonance frequency is shifted, the resonator instantaneously follows the shift. The resonance frequency can be measured by a frequency counter or a timer typically equipped in a data acquisition (DAQ) board. For applications requiring frequency readout exclusively (i.e. buoyant mass measurements), closed loop operation is certainly recommended. However, for applications requiring either amplitude or phase information (i.e. energy dissipation measurements associated traveling particles or viscous solutions), open loop operation is better suited. Of note, open loop operation in this paper is not same as the typical frequency sweep measurement since the operation frequency is fixed near the resonance frequency.

Experimental setup

Figure 3 shows the schematic of our experimental setup for bimodal operation of microchannel resonators where optical readout and electrical control block diagram are exclusively shown (i.e. fluidic interconnections to the microchannel resonator and pneumatic control for particle dynamic trapping [17] are not included herein). The suspended microchannel resonator used in this work is 406 μm long, 28.5 μm wide, and 12 μm tall and exhibits an integrated microchannel that is 8 μm wide and 8 μm tall. The drive and ground electrodes are integrated for electrostatic actuation. In addition to the on-chip electrostatic actuation used for closed loop operation with the first mode, off-chip actuation based on a commercial piezo actuator is added for open loop operation with the

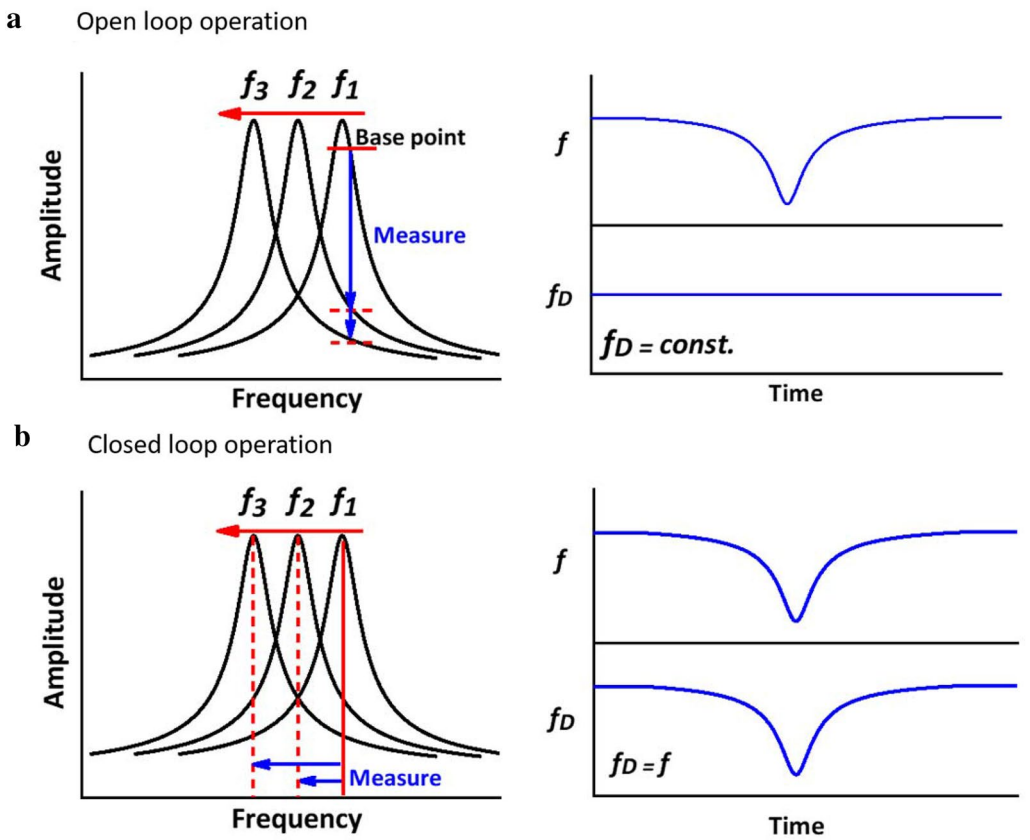

Fig. 2 Open and closed loop operation of mechanical resonators. **a** Amplitude spectrum (left) and drive and measured resonance frequencies (right) during open loop operation. In this mode, amplitude change and phase shift are measured. **b** Amplitude spectrum (left) and drive and measured resonance frequencies (right) during closed loop operation. In this mode, frequency shift is measured

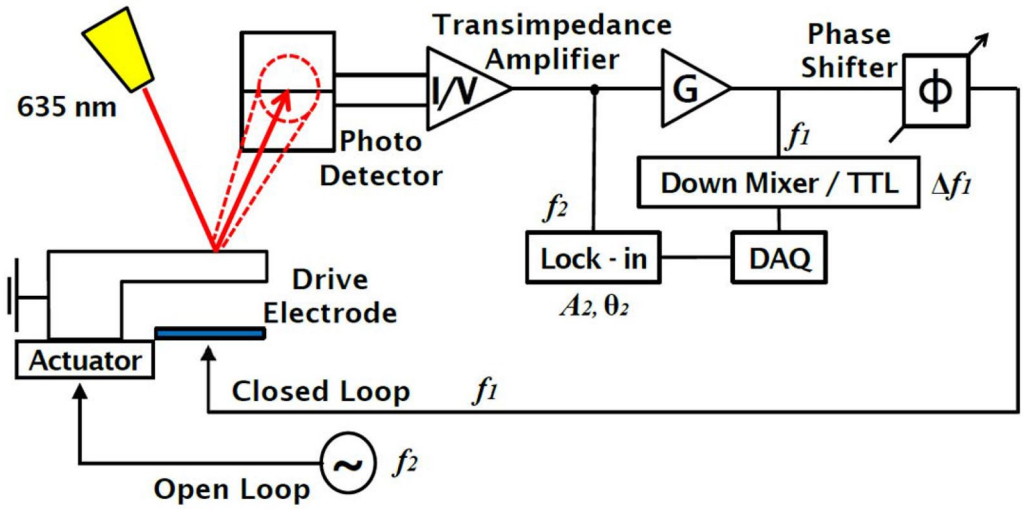

Fig. 3 Schematic of experimental setup. This setup is capable of measuring the frequency shift of the first resonance mode and amplitude change and phase shift of the second resonance mode simultaneously upon transit of a single microparticle through a microchannel resonator

second mode. Once a laser diode reflected off the microchannel resonator is incident on a two-segmented (2-cell) photodiode, AC photocurrent generated is converted into voltage via a transimpedance amplifier. The output from the transimpedance amplifier is further amplified, phase-shifted, and fed back to the on-chip electrostatic actuation electrode. The piezo actuator is separately driven with a constant magnitude at a fixed frequency near the second mode. To measure the first mode resonance frequency, the amplified AC signal is modulated with a reference sine wave from a function generator by a heterodyne down-mixer and then converted into a square wave by a transistor–transistor logic (TTL) level generator. The frequency of the down-modulated square wave is measured by a timer in a DAQ board (National Instruments, USB-6361). To measure amplitude change and phase shift of the second mode, the output from the transimpedance amplifier is measured by a lock-in amplifier (Stanford Research Systems, SR844). For synchronized data logging, outputs from the lock-in amplifier are measured with the same DAQ. This setup is capable of measuring the frequency shift of the first resonance mode and amplitude change and phase shift of the second resonance mode simultaneously upon transit of a single microparticle through a microchannel resonator.

Result and discussion

Bimodal operation is demonstrated with the cantilever-type microchannel resonator and 5-μm diameter single polystyrene particle suspended in deionized water. To evaluate the measurement repeatability by ruling out variation resulting from size distribution, the same polystyrene microparticle is dynamically trapped (i.e. a polystyrene microparticle travels back and forth multiple times) while the microchannel resonator is under bimodal operation. Figure 4 shows resonance frequency shift of the first mode (top), amplitude change (middle) and phase shift (bottom) of the second mode measured simultaneously when a 5-μm diameter single polystyrene particle is dynamically trapped with averaged period of 1.16 s (all three graphs show only 5 transits out of 3500 repeated events). All data are sampled at ~ 2 kHz and then processed by using the Savitzky-Golay filter (3rd order, n = 25) for random noise reduction. As expected from Fig. 1c, the first mode frequency shift shows a single downward peak per each transit and amplitude change and phase shift in the second mode show three upward and downward peaks, respectively.

For statistical comparison, all 3500 transit events are analyzed and plotted as histograms (see Fig. 5). Coefficient of variation (CV), the ratio of the standard deviation to the mean, for the first mode frequency shift is 0.22%. CVs for the second mode amplitude change are 2.03% at the tip and 1.63% at the antinode, respectively. CVs for the second mode phase shift are 2.65% at the tip and 2.56% at the antinode, respectively. Means, standard deviations, and CVs for all cases are summarized in Table 1. The smallest CV for the first mode frequency shift is due to the closed loop feedback operation. Even at the antinode where there is no position error, CVs for the

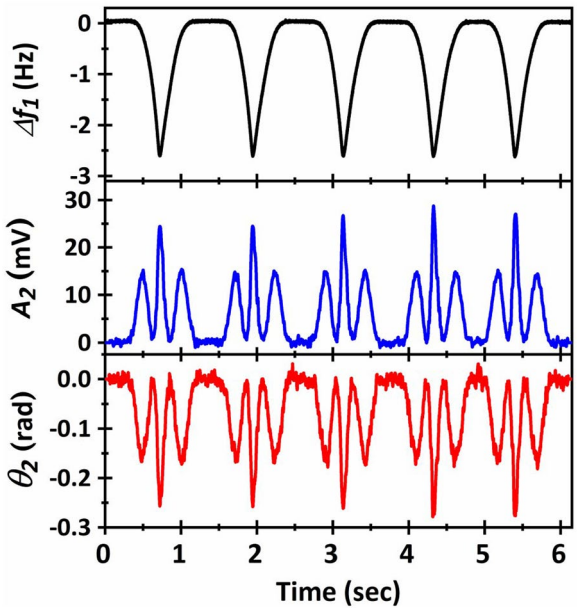

Fig. 4 Bimodal operation of a cantilever-type SMR. Resonance frequency shift of the first mode (top), amplitude (middle) and phase (bottom) changes of the second mode measured when a 5-μm diameter single polystyrene particle is dynamically trapped

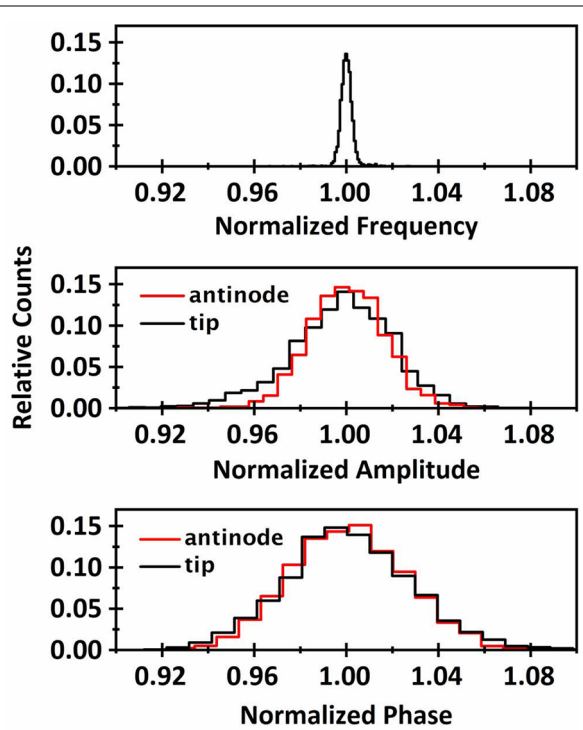

Fig. 5 Histogram comparison. Histograms of the first mode resonance frequency shift (top) and the second mode amplitude (middle) and phase (bottom) changes. All histograms are for 3500 repeated measurements with a same polystyrene microparticle of 5-μm diameter

Table 1 Summary of statistical analysis for repeated measurements

	Mean	Std dev.	CV (%)
Frequency shift (Hz)	2.64	0.0057	0.22
Amplitude change @ tip (mV)	28.7	0.582	2.03
Amplitude change @ antinode (mV)	16.1	0.262	1.63
Phase change @ tip (rad.)	0.275	0.00728	2.65
Phase change @ antinode (rad.)	0.172	0.00441	2.56

Mean, standard deviation (std dev.), and coefficient of variation (CV)

second mode are one order of magnitude larger than the CV for the first mode. This is due to the lock-in detection that requires relatively small actuation magnitude. If the first mode is operated in open loop and the second mode is operated in closed loop, opposite results would be observed. The size of particles is a very important parameter that affects the outputs. When the particle is very small, the volume displaced by the particle is also small. Therefore, the change of effective mass becomes mitigated for a given mass density and energy dissipation originating from the interaction between the particle and surrounding liquid medium is also suppressed. In contrast, when the particle is very large, both the change of effective mass and energy dissipation become significantly increased. However, when the particle diameter becomes larger than 70% of the channel height, the channel resonator tends to be clogged. This clogging issue limits the dynamic range of the channel resonator.

Bimodal operation demonstrated herein will be useful to measure microscale objects with viscoelastic properties and can be applied for two arbitrary modes including flexural and torsional modes. The proposed bimodal operation is not limited to microchannel resonators thus applicable to other types of resonant mass sensors [18] as well as other resonant systems [19].

Conclusions

This paper reports the bimodal operation of microchannel resonators by employing two actuation methods simultaneously to measure properties related with energy dissipation as well as buoyant mass of suspended microparticles. When a 5-μm diameter single polystyrene particle travels back and forth multiple times within the suspended region of microchannel resonators, the first and second flexural modes of microchannel resonators are operated in closed and open loops, respectively. Therefore, the first mode measures resonance frequency shift induced by the particle and the second mode measures amplitude change and phase shift associated with the particle. If the proposed bimodal operation is applied for samples exhibiting viscoelasticity, valuable

information related with dissipation or damping could be effectively investigated.

Acknowledgements
Suspended microchannel resonators were generously provided by the laboratory of Prof. Scott Manalis (MIT, Cambridge, MA).

Authors' contributions
JL developed the idea and performed the experiments. BJL and JL analyzed the results and drafted the manuscript. Both authors read and approved the final manuscript.

Funding
This research was supported by the National Research Foundation of Korea (NRF) funded by the Korea government (Ministry of Science and ICT) (NRF-2017R1A2B3009610).

Availability of data and materials
The datasets used and/or analysed during the current study are available from the corresponding author on reasonable request.

Ethics approval and consent to participate
Not applicable.

Competing interests
The authors declare that they have no competing interests.

Received: 20 April 2019 Accepted: 11 July 2019
Published online: 16 July 2019

References

1. Burg TP, Godin M, Knudsen SM, Shen W, Carlson G, Foster JS, Babcock K, Manalis SR (2007) Weighing of biomolecules, single cells and single nanoparticles in fluid. Nature 446:1066–1069
2. Lee J, Bryan AK, Manalis SR (2011) High precision particle mass sensing using microchannel resonators in the second vibration mode. Rev Sci Instrum 82:023704
3. Olcum S, Cermak N, Wasserman SC, Manalis SR (2015) High-speed multiple-mode mass-sensing resolves dynamic nanoscale mass distributions. Nat Commun 6:7070
4. Martin Y, Williams CC, Wickramasinghe HK (1987) Atomic force microscope force mapping and profiling on a sub 100-Å scale. J Appl Phys 61:4723–4729
5. Albrecht TR, Grutter P, Horne D, Rugar D (1991) Frequency-modulation detection using high-Q cantilevers for enhanced force microscope sensitivity. J Appl Phys 69:668–673
6. Zhong Q, Inniss D, Kjoller K, Elings VB (1993) Fractured polymer silica fiber surface studied by tapping mode atomic-force microscopy. Surf Sci 290:L688–L692
7. Stark RW, Drobek T, Heckl WM (1999) Tapping-mode atomic force microscopy and phase-imaging in higher eigenmodes. Appl Phys Lett 74:3296–3298
8. Garcia R, Perez R (2002) Dynamic atomic force microscopy methods. Surf Sci Rep 47:197–301
9. Lozano JR, Garcia R (2008) Theory of multifrequency atomic force microscopy. Phys Rev Lett 100:076102
10. Garcia R, Herruzo ET (2012) The emergence of multifrequency force microscopy. Nat Nanotechnol 7:217–226
11. Guo SL, Solares SD, Mochalin V, Neitzel I, Gogotsi Y, Kalinin SV, Jesse S (2012) Multifrequency imaging in the intermittent contact mode of atomic force microscopy: beyond phase imaging. Small 8:1264–1269
12. Garcia R, Proksch R (2013) Nanomechanical mapping of soft matter by bimodal force microscopy. Eur Polym J 49:1897–1906
13. Ebeling D, Solares SD (2013) Bimodal atomic force microscopy driving the higher eigenmode in frequency-modulation mode: implementation, advantages, disadvantages and comparison to the open-loop case. Beilstein J Nanotechnol 4:198–207
14. Kiracofe D, Raman A, Yablon D (2013) Multiple regimes of operation in bimodal AFM: understanding the energy of cantilever eigenmodes. Beilstein J Nanotechnol 4:385–393
15. Dietz C, Zerson M, Riesch C, Gigler AM, Stark RW, Rehse N, Magerle R (2008) Nanotomography with enhanced resolution using bimodal atomic force microscopy. Appl Phys Lett 92:143107
16. Athanasopoulou EN, Nianias N, Ong QK, Stellacci F (2018) Bimodal atomic force microscopy for the characterization of thiolated self-assembled monolayers. Nanoscale 10:23027–23036
17. Godin M, Delgado FF, Son SM, Grover WH, Bryan AK, Tzur A, Jorgensen P, Payer K, Grossman AD, Kirschner MW, Manalis SR (2010) Using buoyant mass to measure the growth of single cells. Nat Methods 7:387–390
18. Ko J, Yoon Y, Lee J (2018) Quartz tuning forks with hydrogel patterned by dynamic mask lithography for humidity sensing. Sens. Actuators B-Chem. 273:821–825
19. Ko J, Jarzembski A, Park K, Lee J (2018) Hydrogel tip attached quartz tuning fork for shear force microscopy. Micro Nano Syst Lett 8:6

Publisher's Note